Title	Limit cycles in a digitally controlled buck converter
Authors(s)	Bradley, Mark; Feely, Orla; Teplinsky, Alexey
Publication date	2011-08-29
Publication information	2011 20th European Conference on Circuit Theory and Design (ECCTD) [proceedings]
Conference details	European Conference on Circuit Theory and Design (ECCTD), Linkoping, Sweden, 29-31 Aug. 2011
Publisher	IEEE
Item record/more information	http://hdl.handle.net/10197/3622
Publisher's statement	Personal use of this material is permitted. Permission from IEEE must be obtained for all other uses, in any current or future media, including reprinting/republishing this material for advertising or promotional purposes, creating new collective works, for resale or redistribution to servers or lists, or reuse of any copyrighted component of this work in other works.
Publisher's version (DOI)	10.1109/ECCTD.2011.6043328

Limit Cycles in a Digitally Controlled Buck Converter

Mark Bradley and Orla Feely
School of Electrical, Electronic & Mechanical Engineering,
University College Dublin, Belfield, Dublin 4, Ireland,
Email: mark.bradley@ucdconnect.ie, orla.feely@ucd.ie

Alexey Teplinsky
Institute of Mathematics,
National Academy of Sciences of Ukraine,
Kiev, Ukraine,
Email: teplinsky@imath.kiev.ua

***Abstract*— We describe the mathematical model of a digitally controlled buck converter. This model is an autonomous discrete-time discontinuous piecewise-linear dynamical system in three dimensions. Investigating this system, we find its equilibrium points, describe the shape and size of possible limit cycles (i.e. stable periodic motions), and derive conditions for their existence and non-existence.**

I. Introduction

DC-DC converters are widely used in a variety of power electronics applications, including portable electronics devices and audio amplifiers [1]. The advantages of using digital control over analog control include re-programmability and consequently higher system flexibility, better noise immunity and the possibility of more sophisticated control schemes [1], [2], [3]. The use of digitally controlled switching power converters has attracted considerable research interest in the last number of years [2], however, the dynamics of these converters are not fully understood at present, and the occurrence of limit cycles in converters of this nature is of considerable interest.

Some basic rules for the elimination of the limit cycles which may develop in the system have been proposed in [1], [3], however, these papers use a describing function approach to the problem, in which the non-linearities associated with the A/D and DPWM converters are replaced by transfer functions. Inherent in this approach is the assumption that the signals at the input of the quantizers are approximately sinusoidal, which is not always the case for the limit cycles concerned [3]. In this paper we aim to analyse the behaviour of the system from a nonlinear dynamics perspective, with no such assumption.

II. Mathematical Model

We consider the digitally controlled dc-dc switching power converter from [3] (Fig. 1), where the switching converter is the synchronous buck converter (Fig. 2). The purpose of the latter is to convert the input voltage $V_{\rm in}$ to a smaller output voltage $v \approx V_{\rm in}d$, where d is the duty cycle of switch S_1, and is limited to the range (0,1). S_1 will be closed for time $T_{\rm s}d$ and open for time $(1-d)T_{\rm s}$, where $T_{\rm s}$ is the switching period. S_2 is switched in a complementary fashion to S_1. The reference voltage $V_{\rm ref}$ is the desired output voltage from the system. There are two non-linear blocks in the feedback path, the analog to digital (A/D) converter and the digital pulse-width modulator (DPWM). The error voltage $v_{\rm e} = v - V_{\rm ref}$ is

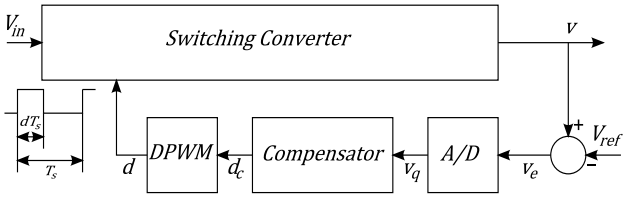

Fig. 1: DC-DC switching power converter from [3]

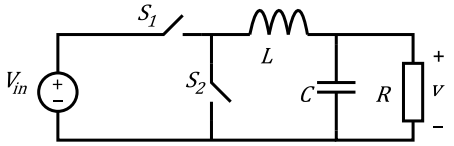

Fig. 2: Synchronous buck converter

sampled and quantized by the A/D converter to give the error signal $v_{\rm q}$. The compensator takes the error signal and produces a corresponding duty-cycle command signal $d_{\rm c}$. This is in turn quantized by the DPWM block to give the duty cycle d, which is applied to the switches in the manner previously described. We shall assume that the frequency at which $v_{\rm e}$ is sampled is equal to the switching frequency $f_{\rm s} = \frac{1}{T_{\rm s}}$, that we sample at the start of a switching period, that there is no quantization in the compensator, and that all circuit components are ideal.

In this situation, the buck circuit is described by

$$\frac{d}{dt}\begin{bmatrix} v(t) \\ i(t) \end{bmatrix} = \begin{bmatrix} -\frac{1}{RC} & \frac{1}{C} \\ -\frac{1}{L} & 0 \end{bmatrix} \cdot \begin{bmatrix} v(t) \\ i(t) \end{bmatrix} + \delta \begin{bmatrix} 0 \\ \frac{1}{L} \end{bmatrix} V_{\rm in}, \quad (1)$$

with $\delta = 1$ for the switch S_1 closed and $\delta = 0$ for S_1 open. Instead of the current i it is convenient to consider the new variable $u = \frac{1}{\omega C} i - \frac{\sigma}{\omega} v$. Denote $W = [v, u]^T$, and (1) becomes

$$\frac{d}{dt} W(t) = AW(t) + \delta \begin{bmatrix} 0 \\ \frac{\omega^2+\sigma^2}{\omega} \end{bmatrix} V_{\rm in} \quad (2)$$

with the constant matrix $A = \begin{bmatrix} -\sigma & \omega \\ -\omega & -\sigma \end{bmatrix}$, where $\sigma = \frac{1}{2RC}$ and $\omega = \sqrt{\frac{1}{LC} - \sigma^2}$. It is not hard to derive that after the equation (2) acts for the time $T_{\rm s}d$ with $\delta = 1$ and then the

time $(1-d)T_\mathrm{s}$ with $\delta = 0$, a starting value W_0 gets transformed into $W_1 = e^{AT_\mathrm{s}}W_0 + N(d)V_\mathrm{in}$, where

$$N(d) = (e^{(1-d)T_\mathrm{s}A} - e^{T_\mathrm{s}A}) \begin{bmatrix} 1 \\ \sigma/\omega \end{bmatrix},$$

and the matrix exponential is given by

$$e^{tA} = e^{-\sigma t} \begin{bmatrix} \cos\omega t & \sin\omega t \\ -\sin\omega t & \cos\omega t \end{bmatrix}, \quad t \text{ real.} \tag{3}$$

We shall use the following equations, modified from [1], to model the feedback system, assuming an integral compensator:

$$d(n) = Q_\mathrm{DPWM}[d_\mathrm{c}(n)], \quad d_\mathrm{c}(n) = -K_\mathrm{i} d_\mathrm{i}(n), \tag{4}$$
$$d_\mathrm{i}(n) = d_\mathrm{i}(n-1) + v_\mathrm{q}(n), \quad v_\mathrm{q}(n) = Q_\mathrm{A/D}[v(n) - V_\mathrm{ref}],$$

where $d = Q_\mathrm{DPWM}[d_\mathrm{c}]$ and $v_\mathrm{q} = Q_\mathrm{A/D}[v_\mathrm{e}]$ are the quantizer functions, which round up their arguments towards the closest values of the form jq_DPWM and $lq_\mathrm{A/D}$ respectively, with j and l integers, for given quantizer steps q_DPWM and $q_\mathrm{A/D}$. We assume Q_DPWM to saturate at some values near 0 and 1, thus there are numbers J_min and J_max such that all values of d_c smaller than $(J_\mathrm{min} + \frac{1}{2})q_\mathrm{DPWM}$ and all values greater than $(J_\mathrm{max} - \frac{1}{2})q_\mathrm{DPWM}$ are rounded towards $J_\mathrm{min}q_\mathrm{DPWM}$ and $J_\mathrm{max}q_\mathrm{DPWM}$ respectively. This forces d to always stay on the segment $[J_\mathrm{min}q_\mathrm{DPWM}, J_\mathrm{max}q_\mathrm{DPWM}] \subset (0,1)$.

We obtain the autonomous three-dimensional discrete-time piece-wise linear discontinuous dynamical system given by:

$$W(n+1) = e^{T_\mathrm{s}A}W(n) + N(d(n))V_\mathrm{in}, \tag{5}$$
$$d_\mathrm{c}(n+1) = d_\mathrm{c}(n) - K_\mathrm{i}v_\mathrm{q}(n+1), \tag{6}$$

with the quantized quantities $d(n)$ and $v_\mathrm{q}(n)$ given by (4). Notice that in this form of the system, the three parameters R, C and L are replaced with only two, namely σ and ω.

The dynamics of this system can be understood as follows. In every particular space layer defined by the quantization level $d_\mathrm{c} \in ((j-\frac{1}{2})q_\mathrm{DPWM}, (j+\frac{1}{2})q_\mathrm{DPWM})$, $J_\mathrm{min} < j < J_\mathrm{max}$, the value of d is equal to $d_j = jq_\mathrm{DPWM}$. The equation (5) can be re-written as $W(n+1) - W_j^* = e^{T_\mathrm{s}A}(W(n) - W_j^*)$, where

$$W_j^* = (I - e^{T_\mathrm{s}A})^{-1}N(d_j)V_\mathrm{in}, \tag{7}$$

so a trajectory in W is a logarithmic spiral winding clockwise towards W_j^* as long as $d = d_j$. Every trajectory thus consists of consecutive spiral segments in W, which are switching their centres (7) in accordance with d_c passing from one quantization level to another. The rate of change of d_c is determined by the quantization level currently occupied by v: d_c is constant as long as v stays inside the *zero error bin* defined by $|v - V_\mathrm{ref}| < \frac{q_\mathrm{A/D}}{2}$, or increases (decreases) as long as v lies to the left (to the right) of that bin.

Obviously, if for some $J_\mathrm{min} \le j \le J_\mathrm{max}$ the point W_j^* lies in the zero error bin, then it represents a fixed point of the system with any $d_\mathrm{c} \in (d_j - \frac{1}{2}q_\mathrm{DPWM}, d_j + \frac{1}{2}q_\mathrm{DPWM})$, and there are no other fixed points. It is of key importance that, due to (3), our system locally uniformly contracts the (v,u)-plane with the coefficient of contraction $e^{-T_\mathrm{s}\sigma}$. It follows that all fixed points and periodic trajectories are asymptotically stable in W. In the sections IV and V we will investigate the fixed points and periodic trajectories of this system in detail. In what follows we assume that the three frequencies involved satisfy the ordering $\sigma \ll \omega \ll 2\pi f_\mathrm{s}$, which is the case for common applications. In particular, this assumption implies the asymptotical equality $W_j^* \approx q_\mathrm{DPWM}V_\mathrm{in}[1, \sigma/\omega]^T j$.

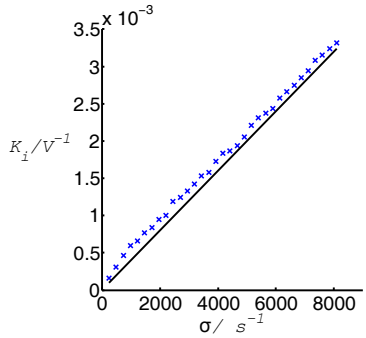

Fig. 3: The crosses show the smallest values of K_i for which a generic trajectory of (5), (6) diverges towards the saturation bounds, the solid line is $K_\mathrm{i}V_\mathrm{in} = 2\sigma T_\mathrm{s}$. Other parameters are $\omega = 98.3$ krad s^{-1}, $T_\mathrm{s} = 10^{-6}$ s, $q_\mathrm{DPWM} = 0.002$, $q_\mathrm{A/D} = 0.101$V, $V_\mathrm{in} = 5$V and $V_\mathrm{ref} = 2.525$V.

III. Continuous System

As the first approximation to the system (5), (6) let us consider a linear autonomous system of differential equations

$$\frac{d}{dt}v(t) = -\sigma v + \omega u, \tag{8}$$
$$\frac{d}{dt}u(t) = -\omega v - \sigma u + \frac{\omega^2 + \sigma^2}{\omega}V_\mathrm{in}d_\mathrm{c}, \tag{9}$$
$$\frac{d}{dt}d_\mathrm{c}(t) = -\frac{K_\mathrm{i}}{T_\mathrm{s}}v + \frac{K_\mathrm{i}V_\mathrm{ref}}{T_\mathrm{s}}, \tag{10}$$

which is obtained from (4), (5) and (6) by removing quantization and linearizing. The system (8)–(10) has a unique fixed point $[V_\mathrm{ref}, \frac{\sigma}{\omega}V_\mathrm{ref}, \frac{V_\mathrm{ref}}{V_\mathrm{in}}]^T$. One of its eigenvalues is real negative and two others are complex conjugate. In order to be stable, the real parts of all eigenvalues have to be negative. An easy calculation results in the *global convergence bound*

$$K_\mathrm{i}V_\mathrm{in} < 2\sigma T_\mathrm{s}. \tag{11}$$

This bound is useful to express the most general information about the system, namely whether $v(n)$ is attracted to some neighborhood of V_ref or repelled from that neighborhood. The numerical comparison of the two systems shows that their dynamics are indeed similar in the large scale. Fig. 3 shows that the bound (11) works well for the discrete system (5), (6).

IV. Fixed Points and Their Regions of Attraction

As previously stated, the discrete system (5), (6) possesses fixed points of the form $[v_j^*, u_j^*, d_\mathrm{c}]^T$, where $[v_j^*, u_j^*]^T = W_j^*$ is given by (7), under the conditions $|d_\mathrm{c} - d_j| < \frac{1}{2}q_\mathrm{DPWM}$, $|v_j^* - V_\mathrm{ref}| < \frac{1}{2}q_\mathrm{A/D}$, $J_\mathrm{min} \le j \le J_\mathrm{max}$. Now we would like to find a region inside the zero error bin in the (v,u)-plane

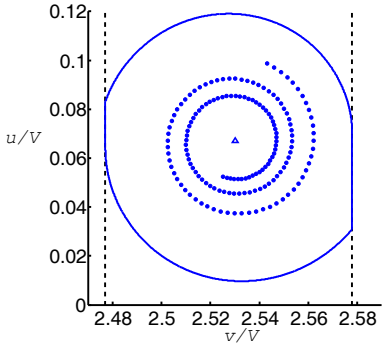

Fig. 4: Attraction to an equilibrium. The parameters are $V_{\rm ref} = 2.5275$ V, $\sigma = 5000$ s^{-1}, $K_{\rm i} = 0.00182$ V^{-1}, others as in Fig. 3. Shown are the equilibrium W^*_{253} (triangle), its region of attraction (bounded by solid line), the zero error bin (bounded by dashed lines) and a piece of trajectory approaching W^*_{253}.

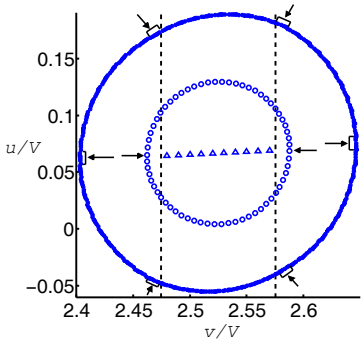

Fig. 5: Co-existing limit cycles and equilibria. Parameters as in Fig. 3, with σ and $K_{\rm i}$ as in Fig. 4. Shown are the equilibria (triangles in the zero error bin), a single-loop limit cycle on two duty-cycle levels (circles), and a 7-loop limit cycle on four levels (solid points). Switching points are marked by arrows.

consisting of points that spiral directly towards W^*_j without any switching. If we assume operation at one duty cycle level d_j, then it is easy to find that $\tilde{W}(n+p) = e^{pT_{\rm s}A}\tilde{W}(n)$, where $\tilde{W}(n) = W(n) - W^*_j$. This relation can be re-arranged into:

$$\tilde{u}\sin p\omega T_{\rm s} + \tilde{v}\cos p\omega T_{\rm s} = \tilde{v}_{\rm bound}e^{p\sigma T_{\rm s}}, \qquad (12)$$

where we consider satisfying a bound $\tilde{v}_{\rm bound}$ in place of $\tilde{v}(n+p)$ as p varies. Once a bound is satisfied for a single turn of a spiral, it will always be satisfied afterwards due to the contraction in W. The sought for region is therefore a polygon bounded by the lines (12) for integer $p \in [0, 2\pi f_{\rm s}/\omega]$ and $\tilde{v}_{\rm bound} = \tilde{v}^{\pm}_{\rm bound} = V_{\rm ref} \pm \frac{1}{2}q_{\rm A/D} - v^*_j$. This region can be approximated by the one bounded by the zero error bin boundaries and two spiral envelopes of the lines (12) given by

$$\tilde{v} = e^{p\sigma T_{\rm s}}\left[\cos p\omega T_{\rm s} - \frac{\sigma}{\omega}\sin p\omega T_{\rm s}\right]\tilde{v}_{\rm bound}, \qquad (13)$$

$$\tilde{u} = e^{p\sigma T_{\rm s}}\left[\sin p\omega T_{\rm s} + \frac{\sigma}{\omega}\cos p\omega T_{\rm s}\right]\tilde{v}_{\rm bound} \qquad (14)$$

with real $p \in [0, 2\pi f_{\rm s}/\omega]$ and $\tilde{v}_{\rm bound} = \tilde{v}^{\pm}_{\rm bound}$ (see Fig. 4).

V. Limit Cycles

Assuming that $q_{\rm DPWM}V_{\rm in} \ll q_{\rm A/D}$, so that there are several fixed points W^*_j inside the zero error bin, the only different kind of limit structures observed in the system (5), (6) are limit cycles, i.e. periodic trajectories, which are locally attracting in the (v,u)-plane, going in an almost circular motion around the fixed point of the continuous system (8)-(10) (which is $v = V_{\rm ref}$, $u = \frac{\sigma}{\omega}V_{\rm ref}$), clockwise at a distance of the order of $q_{\rm A/D}$. The rotation number of such a limit cycle (i.e. the average number of full rotations in one step) is a rational number close to the ratio of the frequencies $\frac{\omega}{2\pi f_{\rm s}} \ll 1$. Limit cycles with different rotation numbers can coexist in the same system (see Fig. 5), similarly to the case studied in [4]. In $d_{\rm c}$, these limit cycles exhibit oscillations over two or more duty-cycle levels.

A. Exact Analysis of Periodic Trajectories

Suppose that from the step $n = n_0$ onwards a trajectory undergoes the sequence $s = (s_1, \ldots, s_K)$ of switchings between duty-cycle levels, spending s_k steps at the duty-cycle level $d = d_{j_k}$, $1 \le k \le K$. If we put $P = \sum_{k=1}^{K} s_k$, then $W(n_0+P) = e^{PT_{\rm s}A}W(n_0) + N_s V_{\rm in}$, where

$$N_s = (I - e^{T_{\rm s}A})^{-1}\sum_{k=1}^{K} e^{T_{\rm s}A\sum_{m=k+1}^{K} s_m}(I - e^{s_m T_{\rm s}A})N(d_{s_m}).$$

Clearly, for this trajectory to be P-periodic, the condition $\sum_{n=1}^{P} v_{\rm q}(n_0+n) = 0$ must be satisfied, and also the actual value of $d(n_0+n)$ has to equal d_{j_k} for $\sum_{m=1}^{k-1} s_m < n \le \sum_{m=1}^{k} s_m$, $1 \le k \le K$. However, due to the complexity of the system, it is impractical to check this large number of conditions. In the next subsections we switch to more informal analysis in order to obtain some practical bounds.

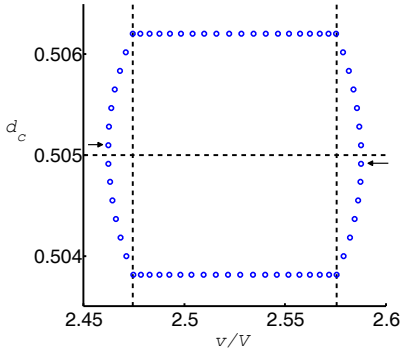

Fig. 6: The single-loop limit cycle on two duty-cycle levels from Fig. 5 in the (v, d_c)-coordinates. The horizontal dashed line divides the $d = d_{252}$ and $d = d_{253}$ duty-cycle levels.

B. Limit Cycles on Two Duty-Cycle Levels

A single-loop limit cycle on two duty-cycle levels (see Fig. 5 and 6) consists (in the (v,u)-coordinates) of two connected pieces of logarithmic spirals, one of which winds around the equilibrium value W^*_j, and the other around its neighbor W^*_{j+1}. Both of these equilibria lie inside the zero error bin, while the two points of switching from one spiral piece to another lie outside. The whole trajectory can be described as

follows. Starting from the left switching point (the one with $v < V_{\rm ref} - \frac{1}{2}q_{\rm A/D}$, $d = d_{j+1}$), the trajectory in the (v,u)-plane goes along the upper spiral piece winding towards W^*_{j+1}, while $d_{\rm c}$ gradually increases until v exceeds $V_{\rm ref} - \frac{1}{2}q_{\rm A/D}$, at which point $d_{\rm c}$ stops changing. With constant $d_{\rm c}$, the trajectory in (v,u) continues along the upper spiral piece until v exceeds $V_{\rm ref} + \frac{1}{2}q_{\rm A/D}$, at which point $d_{\rm c}$ starts to decrease, and further to the right switching point, at which $d_{\rm c}$ falls below $(j+1/2)q_{\rm DPWM}$ so that d becomes d_j. Then the similar dynamics carry the trajectory back to the left switching point along the lower spiral piece winding towards W^*_j. The period of this trajectory is an integer close to $\frac{2\pi f_{\rm s}}{\omega}$. A multiple-loop limit cycle differs from a single-loop one in that the above-described dynamics do not carry the trajectory to its starting point after just one loop, so it switches again at a different point to the left of the zero error bin and then proceeds to yet another switching point to the right, returning to the starting point after making several loops close to each other.

Three conditions are necessary for such a limit cycle to be realizable in a particular system. First of all, the total excursion of this limit cycle in v has to be greater than the width of the zero error bin, so that the switching points on both sides can lie outside that bin. Assuming that the switching points as well as the equilibria W^*_j and W^*_{j+1} lie approximately on the same horizontal line in the (v,u)-plane, one can estimate that the excursion of the limit cycle in v is given by

$$\frac{1+e^{-\frac{\pi\sigma}{\omega}}}{1-e^{-\frac{\pi\sigma}{\omega}}} q_{\rm DPWM} V_{\rm in} \approx \frac{2\omega}{\pi\sigma} q_{\rm DPWM} V_{\rm in}. \tag{15}$$

Generically, the excursion is slightly smaller than (15), since the four points do not lie exactly on the same horizontal line. This estimate is close to the one obtained in [3]. Thus, one necessary condition for a limit cycle on two duty-cycle levels to exist is that the excursion in v is greater than $q_{\rm A/D}$, i.e.

$$\frac{q_{\rm DPWM} V_{\rm in}}{q_{\rm A/D}} > \frac{\pi\sigma}{2\omega}. \tag{16}$$

The second condition is some degree of symmetry in the system, although it does not have to be exact. As the equilibria are proportional to $V_{\rm in}$, a small change in that value would easily break or create such a symmetry. Therefore, if our aim is to avoid the limit cycles without knowing the input voltage exactly, we have to assume the worst case, i.e. that the symmetry is present.

The third condition is an upper bound on the gain $K_{\rm i}$. It is necessary because the excursion of $d_{\rm c}$ cannot exceed $2q_{\rm DPWM}$, otherwise there would be more than two duty-cycle levels involved. The greatest possible value of $K_{\rm i}$ for a given shape of the limit cycle in the (v,u)-plane depends on how many steps are spent by the trajectory beyond the zero error bin. If there are N_m steps on the mth quantization level, $m \geq 1$, then the bound $K_{\rm i} < 2\frac{q_{\rm DPWM}}{q_{\rm A/D}}(\sum_m mN_m)^{-1}$ has to hold.

C. Limit Cycles on More Than Two Duty-Cycle Levels

Limit cycles on $D \geq 3$ duty-cycle levels look similar to the two-level ones in that their trajectory in (v,u) rotates clockwise around $(V_{\rm ref}, \frac{\sigma}{\omega}V_{\rm ref})$ with somewhat greater amplitude. In fact its circular shape consists of spiral pieces having more than two switching points along each loop. In order to find a rough bound on the minimum value of $K_{\rm i}$ for which a limit cycle on $D > 2$ levels may occur, we consider a limit cycle confined to the ± 1 and 0 error bins. In this case, there will be $(D-1)$ switching points in each of the ± 1 error bins, and we assume that the angle spent in each of these bins is given by $(D-2)\alpha_{\rm D}$. For a limit cycle on D levels to exist, its excursion in $d_{\rm c}$ must be at least $(D-2)q_{\rm DPWM}$, yielding

$$K_{\rm i} > \frac{q_{\rm DPWM}}{q_{\rm A/D}} \frac{\omega T_{\rm s}}{\alpha_{\rm D}} \tag{17}$$

Omitting the calculations, we find the following approximate relation

$$\frac{\sin\left((D-1)\,\frac{\alpha_{\rm D}}{2}\right)\cos\left((D-2)\,\frac{\alpha_{\rm D}}{2}\right)}{\sin\left(\frac{\alpha_{\rm D}}{2}\right)} = \frac{q_{\rm A/D}}{q_{\rm DPWM} V_{\rm in}} \frac{\pi\sigma}{2\omega} \tag{18}$$

Considering the curves from the LHS of (18) for different values of D, $\alpha_{\rm D}$ will be the largest angle in the range $\frac{\pi}{2(D-2)} < \alpha_{\rm D} < \frac{\pi}{2(D-1)}$. Correspondingly, we have

$$\frac{1}{\sqrt{2}} \frac{\cos\left(\frac{D-2}{D-1}\,\frac{\pi}{4}\right)}{\sin\left(\frac{1}{D-1}\,\frac{\pi}{4}\right)} < \frac{q_{\rm A/D}}{q_{\rm DPWM} V_{\rm in}} \frac{\pi\sigma}{2\omega} < \frac{1}{\sqrt{2}} \frac{\sin\left(\frac{D-1}{D-2}\,\frac{\pi}{4}\right)}{\sin\left(\frac{1}{D-2}\,\frac{\pi}{4}\right)} \tag{19}$$

D. No-Limit-Cycles Condition

The main objective of this work is establishing conditions which would guarantee that no limit cycles exist in the system. A sufficient no-limit-cycles condition is for the two bounds

$$\frac{q_{\rm DPWM} V_{\rm in}}{q_{\rm A/D}} < \frac{\pi\sigma}{2\omega}, \quad K_{\rm i} < \frac{q_{\rm DPWM}}{q_{\rm A/D}} \frac{\omega T_{\rm s}}{\alpha_{\rm D}}, \tag{20}$$

to hold simultaneously, where $\alpha_{\rm D}$ is the angle from (18), with D, $q_{\rm DPWM}$, $q_{\rm A/D}$ and ω satisfying the relation in (19).

VI. Conclusions

A mathematical model of a digitally controlled buck converter was presented. A continuous model of the system was described and a bound for global convergence of the system was derived. The steady-state dynamical patterns of the system, fixed points and limit cycles, were investigated and conditions for the existence of limit cycles were derived. A no-limit-cycle condition for the system was then discussed.

Acknowledgments

Mark Bradley acknowledges the support of the Irish Research Council for Science, Engineering and Technology.

References

[1] A. V. Peterchev and S. R. Sanders, "Quantization resolution and limit cycling in digitally controlled pwm converters," *IEEE Trans. Power Electron.*, vol. 18, no.1, pp. 301–308, 2003.

[2] Y.-F. Liu, E. Meyer, and X. Liu, "Recent developments in digital control strategies for dc/dc switching power converters," *IEEE Trans. Power Electron.*, vol. 24, no. 11, pp. 2567–2577, 2009.

[3] H. Peng, D. Maksimovic, A. Prodic, and E. Alarcon, "Modeling of quantization effects in digitally controlled dc-dc converters," *IEEE Trans. Power Electron.*, vol. 22, no. 1, pp. 208–215, 2007.

[4] A. Teplinsky and O. Feely, "Limit cycles in a mems oscillator," *IEEE Trans. Circuits Syst. II*, vol. 55, no. 9, pp. 882–886, 2008.